https://doi.org/10.30799/jnst.152.18040505 J. Nanosci. Tech. - Volume 4 Issue 5 (2018) 478–482

ISSN: 2455-0191

Share Your Innovations through JACS Directory

Journal of Nanoscience and Technology

Visit Journal at http://www.jacsdirectory.com/jnst

Synthesis and Characterization of Pure and Rare-Earth Metal Gd Doped SnO_2-CuO Nanoparticles by Co-Precipitation Method

L. Prakash, C. Tirupathi*

PG and Research Department of Physics Sacred Heart college (Autonomous), Tirupattur, Vellore - 635 601, Tamil Nadu, India.

ARTICLEDETAILS

Article history:
Received 16 August 2018
Accepted 24 August 2018
Available online 30 August 2018

Keywords:
Gd Doped SnO_2-CuO
Dielectric Studies
Co-precipitation Method

ABSTRACT

Pure and rare-earth metal Gd doped SnO_2-CuO nanoparticles were successfully prepared from the starting materials $SnCl_2$, $CuCl_2$ and doping element gadolinium nitrate. Pure and Gd doped SnO_2-CuO were synthesized by co-precipitation method. The samples were characterized using X-ray diffraction (XRD), Fourier transformed infrared spectroscopy (FTIR), UV-Vis, SEM, EDX and dielectric studies. The XRD analysis reveals that the rare-earth metal Gd dopants were substituted into rutile SnO_2-CuO nanoparticles. Pure SnO_2-CuO nanoparticles have an average crystallite size of 15 nm and rare-earth metal Gd doped SnO_2-CuO nanoparticles have 18 nm. The average crystallite size of the sample increases when dopant was used and XRD peak intensity also increases when compared to pure SnO_2-CuO nanoparticles. The optical absorption measurements exposed the nanometric size of the materials influences the energy band gap. Optical band gap was found to be 5.08 eV for pure SnO_2-CuO nanoparticles and 5.14 eV for Gd doped SnO_2-CuO nanoparticles. Surface morphology of pure and Gd doped SnO_2-CuO nanoparticles annealed at 400 °C shows that most of the particles are rod shaped and hence it may have better sensitivity. Dielectric constant and dielectric loss decrease with increasing frequency at 100 °C and 200 °C. Doped samples show larger dielectric properties than pure SnO_2-CuO nanoparticles.

1. Introduction

Nanomaterials are having excellent chemical and physical properties because of their smaller grain size, high surface area, quantum confinement effect and high sintering ability. Copper oxide (CuO) is an important material due to its high dielectric constant and P-type semiconductor and band gap value in the range of 1.8 eV - 2.5 eV. They are suitable material for giant efficiency solar cells because their band gap value is close to the prefect energy gap for solar cells [1, 2]. Copper oxide nanomaterials are widely used in various applications such as magnetic storage media**,** solar cell technology, gas sensing, field emission, [3-5] etc. Tin oxide (SnO_2) is n- type semiconductor with their band gap value in the range of 3.3 eV -3.6 electron volt and it has a broad range of applications in gas sensors, catalysts, optoelectronic devices, transparent conducting electrodes [6-8], dye-sensitized solar cells [9-12], negative electrodes for lithium batteries [13-15], panel displays, etc. It is basically notice that by increasing the surface to volume ratio by decreasing the grain size of tin oxide is crucial for achieving giant sensitivity in applicable of gas sensors [16]. High sensitivity of the electrical conduction of SnO_2, support these conductive oxides for the detection of flammable gases in air [17-19]. Recently, rare-earth metal (Gd) doped dilute magnetic semiconductor (DMS) materials attract interest among the researchers because of their unique optical properties and high emission quantum yield. The rare-earth Gd ion is doped to metal oxides were found applicable for spintronics applications. In particular, nowadays experimental results have been shown that the embodiment of rare-earth metals such as Gd ion in broad band gap semiconductor. Gd^{3+} ion is one of the greatest interest due to its application in scintillation and optical devices in the place of other luminescent and large magnetic behaviour materials [20-22]. The SnO_2-CuO nanoparticles having a subject of must importance because of its outstanding physical and chemical properties and a workable future dielectric material for no of functional devices. The pure and rare-earth metal (Gd) doped SnO_2-CuO nanoparticles have enjoyed most well-liked nanoparticles and their increasing interest to an oversized quantity of their valuable applications in numerous fields, particularly the potential application of SnO_2-CuO in insulators and sensing powerfully connected with dominant of their size and morphology by the correct alternative of preparation conditions. We are going to improve their special behaviour using doping, the Gd ions is very much suitable for SnO_2-CuO depend on their high dielectric behaviour, controlled size and morphology [23, 24]. The synthesis of pure and Gd doped SnO_2-CuO nanoparticles calculated by co-precipitation method are very much convenient, as they are economical. Nanoparticle solutions obtained are relatively stable and yield high amount of powder. Our aim of this work is to exploration the dielectric properties of pure and Gd doped SnO_2-CuO nanoparticles. This work have studied the temperature and frequency dependence of dielectric constant. Also, we have discussed the dielectric loss, conductivity, resistivity, band gab energy and crystallite size of pure and Gd doped SnO_2-CuO nanoparticles.

2. Experimental Methods

2.1 Preparation of Pure SnO_2-CuO Nanoparticles

Pure SnO_2-CuO nanoparticles were synthesized via chemical co-precipitation method. High purity AR grade chemical reagents, $SnCl_2{\cdot}2H_2O$ (98.8%) and $CuCl_2{\cdot}2H_2O$ (98.7%), distilled water and ammonia solution, were used for the synthesis. In the typical synthesis $SnCl_2{\cdot}2H_2O$ (98.8%) and $CuCl_2{\cdot}2H_2O$ (98.7%) precursors in 1:1 molar ratio was mixed and stirred for 1 hr. In addition, small amount of ethylene glycol (8–10 mL) was added as capping representative. The magnetic stirring was done for 24-25 hr to make certain complete and intimate reaction between different compounds. Ammonia solution (NH_3) was added to above mixture drop by drop. The product was dried for 3.30 hrs at 90 °C in hot oven and calcined at 400 °C for 5 hr, resulting at complete crystallization to obtain SnO_2-CuO nanoparticles in powder form. The final product was pale green in colour (Fig. 1(a)). Afterwards the sample was characterized with wide angle x-ray phase analysis XRD, FT-IR analysis, UV-visible analysis, dielectric analysis, SEM analysis and EDX.

2.2 Preparation of Rare- Earth Metal Gd Doped SnO_2-CuO Nanoparticles

Rare-earth metal Gd doped SnO_2-CuO nanoparticles were synthesized via chemical co-precipitation method. High purity AR grade chemical

*Corresponding Author:thirupathy@shctpt.edu(C. Tirupathi)

https://doi.org/10.30799/jnst.152.18040505

Cite this Article as: L. Prakash, C. Tirupathi, Synthesis and characterization of pure and rare-earth metal Gd doped SnO_2-CuO nanoparticles by co-precipitation method, J. Nanosci. Tech. 4(5) (2018) 478–482.

reagents, $SnCl_2{\cdot}2H_2O$ (98.8%) ($CuCl_2{\cdot}2H_2O$ (98.7%), $GdNO_3{\cdot}2H_2O$ (99.8%), distilled water and ammonia solution, were used for the synthesis. In the typical synthesis $SnCl_2{\cdot}2H_2O$ (98.8%) and $CuCl_2{\cdot}2H_2O$ (98.7%) precursors in 1:1 molar ratio were mixed and stirred for 1 hr. Afterwards gadolinium nitrate ($GdNO_3{\cdot}2H_2O$) was added and stirred for 6 hr in order to ensure doping of gadolinium into SnO_2-CuO. In addition, small amount of ethylene glycol (8–10 mL) was mixed as capping representative. The magnetic stirring was done for 24-25 hr to make certain complete and intimate reaction between different compounds. Ammonia solution (NH_3) was added to above mixture drop by drop. The product was dried for 3.30 hrs at 90 °C in hot oven and calcined at 400 °C for 5 hr, resulting at complete crystallization to obtain gadolinium doped SnO_2-CuO nanoparticles in powder form. The final product was brown in colour (Fig. 1(b)). Afterwards the sample was characterized with wide angle x-ray phase analysis XRD, FT-IR analysis, UV-visible analysis, dielectric analysis, SEM analysis and EDX.

Fig. 1 (a) Pure SnO_2-CuO nanoparticles and (b) Gd doped SnO_2-CuO nanoparticles

3. Results and Discussion

3.1 X-Ray Diffraction Patterns (XRD)

XRD pattern of pure and rare-earth metal Gd doped SnO_2-CuO nanoparticles prepared via co-precipitation method and calcined at 400 °C are shown in Fig. 2. All the diffraction peaks of XRD with 2θ at 14.01° (0 0 2), 16.06° (0 1 1), 17.04° (2 0 0), 21.07° (1 1 0), 33.07° (1 0 1), 40.12° (1 1 1), 55.08° (2 0 2), 57.13° (3 1 0) belong to orthorhombic structure of SnO_2. The calculated lattice parameters of SnO_2 are a = 3.823 Å, b= 3.610 Å, c = 4.30 Å, and these data are in well coincidence with the already reported values (JCPDS file no. 24-1342). The diffraction of intensity peaks of XRD with 2θ at 29.03° (1 1 1), 36.08° (2 0 0), 45.32° (1 1 2), 47.08° (0 2 0), 50.03° (2 0 0) belong to monoclinic structure of CuO. The calculated lattice parameters of CuO are a= 4.688 Å, b=3.422 Å, c= 5.131 Å, and these values are well coincidence with the reported values (JCPDS file no. 48-1548). And the diffraction peaks of XRD with 2θ at 31.14° (2 0 0), 47.09° (2 2 0) belong to cubic structure of GdO. The calculated lattice parameters of GdO are a = b = c = 5.400 Å and these data are well pact with the already reported values (JCPDS file no. 73-2403). The crystallite sizes were calculated using Debye Scherrer's formula. The crystallite size of pure SnO_2-CuO nanoparticles is found to be 15 nm and rare-earth metal Gd doped SnO_2-CuO nanoparticles is forms to be 18 nm.

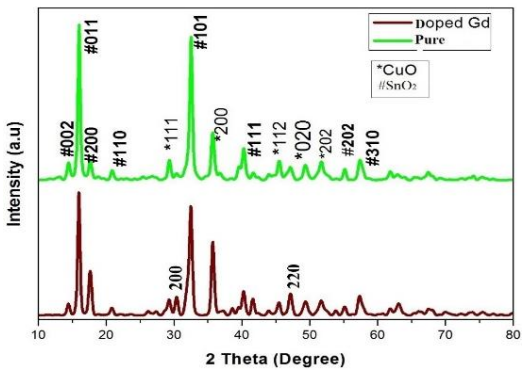

Fig. 2 XRD pattern of pure and doped rare-earth metal Gd doped SnO_2-CuO nanoparticles

3.2 FTIR Spectrometer Analysis

FT-IR spectra of the particular functional group of vibration pure and Gd doped SnO_2-CuO nanoparticles prepared via co-precipitation method and calcined at 400 °C are shown in Fig. 3. The peak at 444 cm^{-1} was due to the vibrations of O-Sn-O [25]. The razor peak at 504 cm^{-1} is because of the Cu-O vibrations [26]. The peak at 540 cm^{-1} is responsible of the Gd-O bond vibrations [27]. Remaining peaks at 1607 and 3402 cm^{-1} was due to absorption of water (H-O-H) vibration) during preparation of KBR pellet.

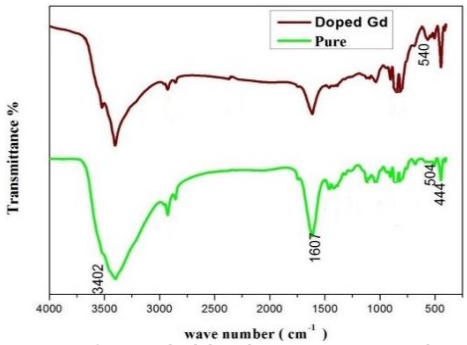

Fig. 3 FT-IR spectrum of pure and Gd doped SnO_2-CuO nanoparticles

3.3 UV-Visible Analysis

UV-visible absorption spectrum of pure and Gd doped SnO_2-CuO nanoparticles prepared via co-precipitation method and calcined at 400 °C are shown in Fig. 4. The maximum absorption was found in ultraviolet region at 244 and 241 nm. This data was further used for analysing optical band gap energy (Eg). The calculated band gab energy of pure SnO_2-CuO nanoparticles are 5.08 eV, rare-earth metal Gd doped SnO_2-CuO nanoparticles are 5.14 eV. This suggests that rare-earth metal Gd doped SnO_2-CuO nanoparticles have an increased band gab energy.

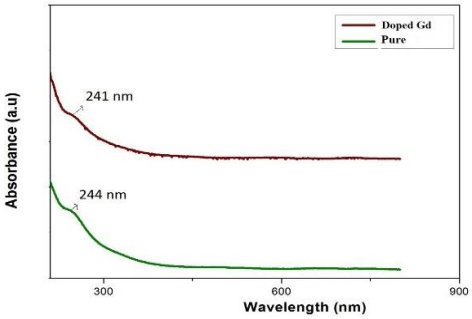

Fig. 4 The absorption spectrum of pure and Gd doped SnO_2-CuO nanoparticles

3.4 Impedance Analysis

3.4.1 Dielectric Constant

The dielectric constant analysis of pure and Gd doped SnO_2-CuO nanoparticles was convey out by using by Impedance Analyzer - PSM 1735 in the temperature range of 30-600 °C and a frequency range of 10 μHz-35 MHz. Dielectric constant was calculated by,

$$\varepsilon_r = C * \frac{d}{\varepsilon_0} A$$

where, ε_0 is the dielectric permittivity of vacuum (8.854 x 10-12 F/m). C is capacitance, A is the area of cross section of the sample, d is the thickness of the sample, and ε_r is the relative permittivity of the material which is a dimensionless quantity.

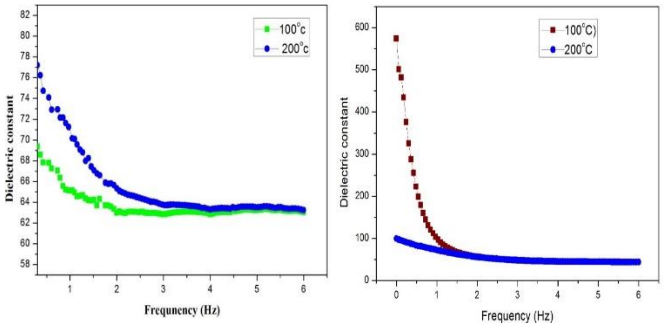

Fig. 5 Dielectric constant vs frequency (logF) of (a) synthesized pure and (b) Gd-SnO_2-CuO nanoparticles

Fig. 5 shows the dielectric constant of pure and Gd doped SnO_2-CuO nanoparticles for varying frequency at 100 °C and 200 °C. It is very clear that dielectric constant seems to be frequency dependent. Also, dielectric

https://doi.org/10.30799/jnst.152.18040505

Cite this Article as: L. Prakash, C. Tirupathi, Synthesis and characterization of pure and rare-earth metal Gd doped SnO_2-CuO nanoparticles by co-precipitation method, J. Nanosci. Tech. 4(5) (2018) 478–482.

constant decreases with increase in frequency (logF). However, while increasing temperatures the dielectric constant also increases because of the well conducting grains and high conducting boundaries. The dielectric constant of pure SnO_2-CuO nanoparticles from the Fig. 5(a) exhibits higher dielectric constant at low frequency and at high frequency region dielectric constant remains static. Whereas, the dielectric constant for Gd doped SnO_2-CuO nanoparticles shows a rapid increase at lower frequencies for 100 °°C but the dielectric constant at 200 °C showed a gradual decrease with increasing frequency. This can be attribute due to impact of doping Gd that accumulates charge carrier around the grains.

3.4.2 Dielectric Loss (tan δ)

The Fig. 6 shows the dielectric loss (tan δ) versus frequency at 100 °C and 200 °C of pure and Gd doped SnO_2-CuO nanoparticles. From Fig. 6(a) pure SnO_2-CuO exhibited high dielectric loss at lower frequencies (0-1 MHz). On further increasing the temperature, dielectric loss remains constant, similar behaviour is observed in rare-earth metal Gd doped SnO_2-CuO nanoparticles. However dielectric loss of gadolinium doped SnO_2-CuO shows static loss above 1.6 MHz which can be due to the impurities such as lattice defects and moisture present in the synthesized compound. Dielectric loss goes to low (very much small) which reveals that material can be used for storing large no of charge without much energy loss. The dielectric loss decreases with increasing frequency which indicate that material has minimum defects and it cans be used for photonic and electro-optic devices application.

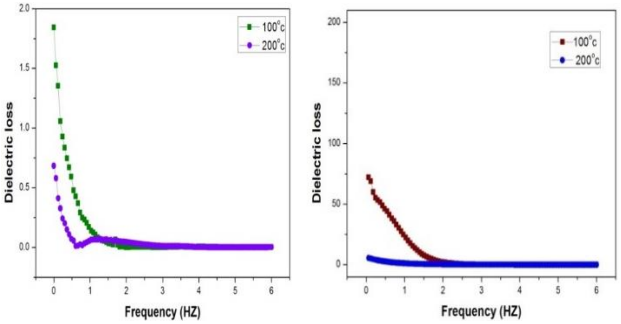

Fig. 6 Tangential loss (dielectric loss) vs frequency of (a) synthesized pure and (b) Gd doped SnO_2-CuO nanoparticles

3.4.3 Resistivity

Fig. 7 shows the discrepancy of resistivity as a function of frequency at 100 °C and 200 °C of pure and Gd doped SnO_2-CuO nanoparticles. It clear that from Fig. 7 resistivity depends on the frequency and by increasing the value of frequency, the resistivity decreases for pure SnO_2-CuO at 100 °C and 200 °C, whereas the resistivity of rare-earth metal Gd doped SnO_2-CuO shows a higher resistivity at 200 °C which may be related to the lower conduction behaviour generated by the dopant. Therefore, rare-earth metal Gd doping ensures less conduction compared to pure SnO_2-CuO.

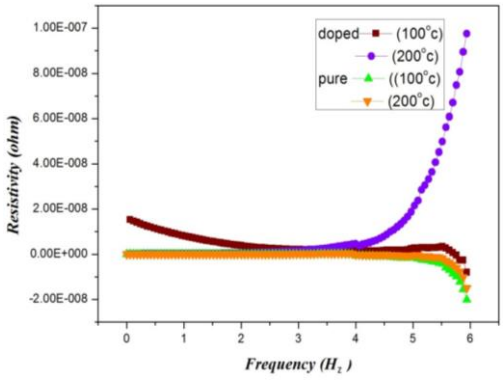

Fig. 7 resistivity vs frequency of synthesized pure and Gd doped SnO_2-CuO nanoparticles

3.4.4 Electrical Permittivity

Based on the impedance, the real, imaginary part of complex relative permittivity can be calculated as follows:

$$\varepsilon' = \frac{z''}{2\pi f c_0 z^2} \quad (1)$$

$$\varepsilon'' = \frac{z'}{2\pi f c_0 z^2} \quad (2)$$

$$c_0 = \varepsilon_o \frac{A}{d} \quad (3)$$

where, c_o = the geometric capacity, A= the area, d= the thickness of the specimen under the investigation. ε_o is the permittivity of the vacuum (8.85×10^{-12} Fm^{-1}). The real and imaginary part of permittivity catalogue the energy loss of dielectrics. The deficiency of a dielectric loss peak in the imaginary part of the permittivity in Fig. 8 indicates the absence of dipolar relaxation processes. The real part of the permittivity vs frequency (logF) and imaginary part of permittivity vs frequency (logF) at temperatures 100 °C and 200 °C are shown in the Fig. 9. For all the samples, both at 100 °C and 200 °C, the real part of permittivity decreases gradually and reaches a constant value after 1 MHz. The permittivity of Gd doped SnO_2-CuO samples is high at 200 °C when compared to that at 100 °C.

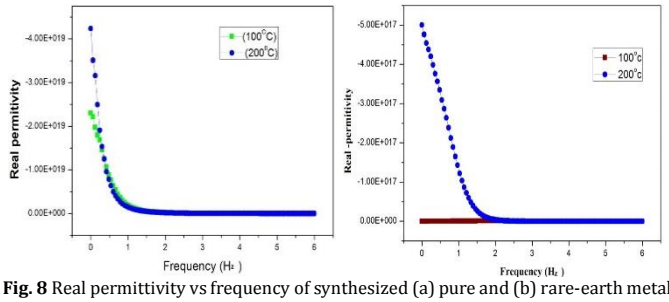

Fig. 8 Real permittivity vs frequency of synthesized (a) pure and (b) rare-earth metal Gd doped SnO_2-CuO nanoparticle

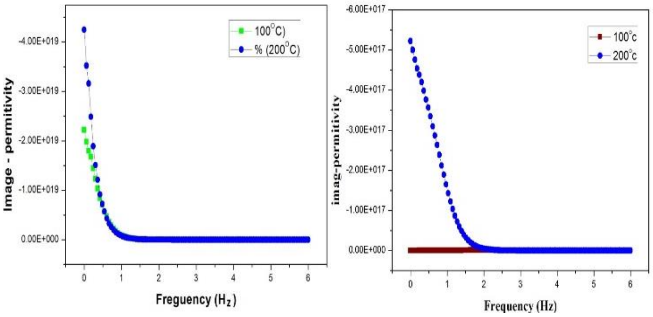

Fig. 9 Image-permittivity vs frequency of synthesized (a) pure and (b) rare-earth metal Gd doped SnO_2-CuO nanoparticles

3.4.5 Conductivity

The electrical conductivity of pure and Gd doped SnO_2-CuO nanoparticles are presented in Fig. 10. The electrical conductivity of rare-earth metal Gd doped SnO_2-CuO nanoparticles in Fig. 10(a) shows that electrical conductivity remains static at low frequency whereas at higher frequencies the conductivity reduces considerably. Fig. 10(b) shows electrical conductivity of pure SnO_2-CuO nanoparticles in which the electrical conductivity is dependent on frequency (logF). In the toll frequency region, conductivity is zero whereas at low frequency (4 MHz), conductivity increases at 200 °C. Therefore, the conductivity is more at 200 °C.

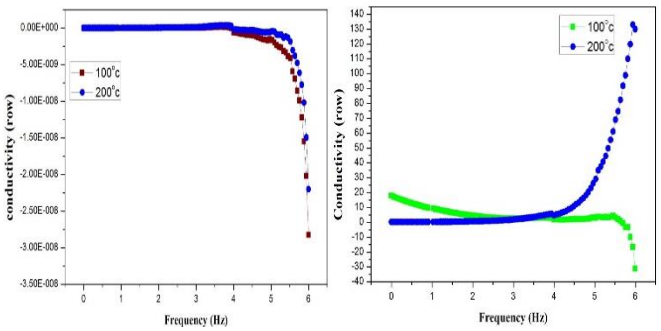

Fig. 10 Conductivity vs frequency of synthesized (a) pure and (b) rare-earth metal Gd doped SnO_2-CuO nanoparticles

3.4.6 Impedance Analysis

Impedance spectroscopy is the approach which is used to disparate by the real and imaginary part of the electrical parameter to reveal the

https://doi.org/10.30799/jnst.152.18040505

Cite this Article as: L. Prakash, C. Tirupathi, Synthesis and characterization of pure and rare-earth metal Gd doped SnO_2-CuO nanoparticles by co-precipitation method, J. Nanosci. Tech. 4(5) (2018) 478–482.

material's electrical properties. Usually the grain barriers are effective offering more impedance in the low frequency (logF). The impedance analysis spectrum of pure and rare-earth metal Gd doped SnO_2-CuO nanoparticles have been studied over a wide range of frequency (1 kHZ-30 MHz). The plot between the real and imaginary part of impedance is called as the Nyquist plots. Fig. 11 shows the Nyquist plots of the Gd doped SnO_2-CuO nanoparticles. Gd doped SnO_2-CuO nanoparticles show semicircle slightly moving into double at high frequency region. The Gd doped SnO_2-CuO nanoparticles show single semicircle like pattern for 100 °C. Here Fig. 11(b) shows that at 200 °C the diameter of the semicircle increase means that these is a change in the resistive element of the material and which is indicating the presence of polarization with a single relaxation time. The radius of the semicircle decreases with the increases in Gd doped SnO_2-CuO. Fig. 12 shows the Nyquist plots of the pure SnO_2-CuO nanoparticles. For both 100 °C and 200 °C, the pure SnO_2-CuO nanoparticles shows an increasing pattern and then decreases as can be witnessed from Fig. 12.

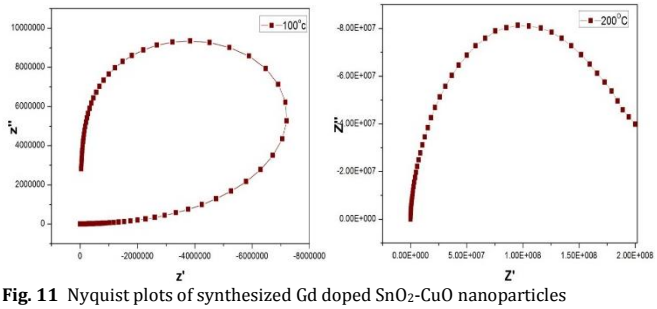

Fig. 11 Nyquist plots of synthesized Gd doped SnO_2-CuO nanoparticles

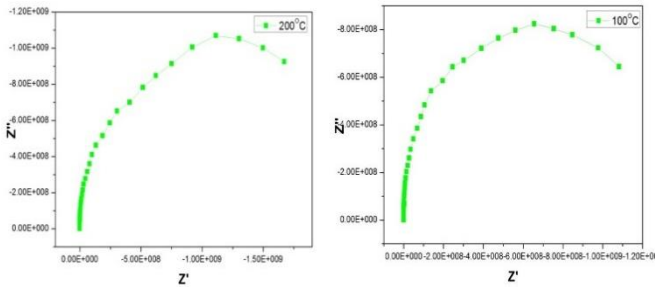

Fig. 12 Nyquist plots of synthesized pure SnO_2-CuO nanoparticles

Fig. 13 shows the discrepancy of real and imaginary part of impedance with various frequency (logF) for Gd doped SnO_2-CuO nanoparticles at 100 °C and 200 °C. It is observed that at low frequency region the Z' values are high at 200 °C and high frequency region the Z' values continuously decrease and merge together. The height of the peak also decreasing with rising in temperature which says the presence of temperature depends relaxation process in the particular given system. The relaxation process because of the presence of static species at minor temperature and defects at huge temperature. This trend shows that the conductivity values are high at larger frequency (logF) region.

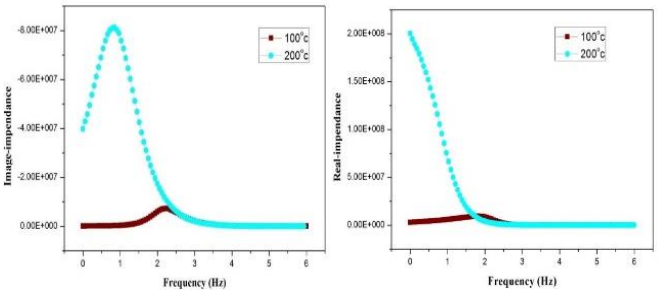

Fig. 13 Image and Real part of impendence vs frequency of synthesized Gd doped SnO_2-CuO nanoparticles

Fig. 14 shows the discrepancy of real and imaginary part of impedance with various frequency for pure SnO_2-CuO nanoparticles at 100 °C and 200 °C. We can clearly say the peak behaviour of real part and image part of impedance values from Fig. 14. There is no large difference in the behaviour of the samples when the temperature is increased from 100 °C to 200 °C. There is a slight variation in values at the lower frequency end which gradually reduces and the curves merge together at high frequency region. The merging of the real & imaginary part of impedance values at higher frequency (logF) denotes for dominant contribution from grain border line.

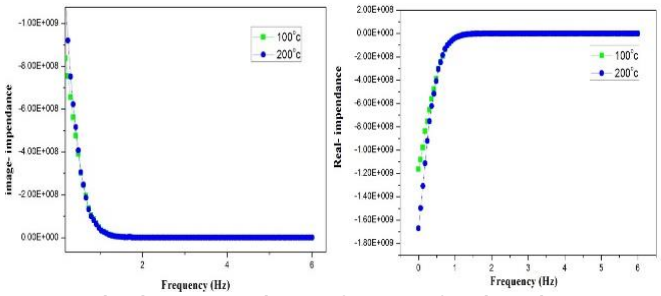

Fig. 14 Real and image-impendence vs frequency of synthesized pure SnO_2-CuO nanoparticles

3.5 SEM-Analysis

3.5.1 Pure SnO_2-CuO Nanoparticles

Fig. 15 shows SEM image of pure SnO_2-CuO nanoparticles. The rod like morphologies are witnessed for pure SnO_2 -CuO nanoparticles calcinate at 400 °C. The average piece size is obtained from SEM investigation is 21 nm.

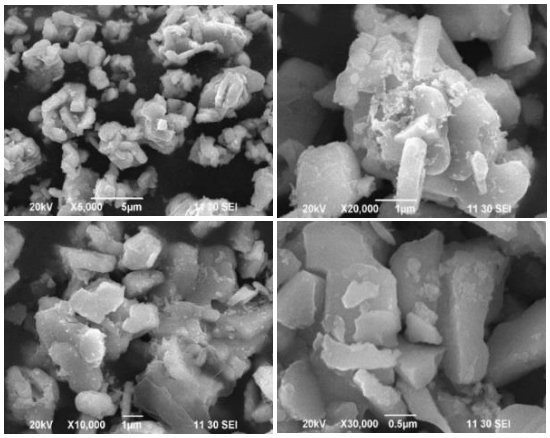

Fig. 15 SEM images of pure SnO_2-CuO nanoparticle

3.5.2 Gd Impurities of SnO_2-CuO Nanoparticles

Fig. 16 shows SEM image of Gd doped SnO_2-CuO nanoparticles calcinated at 400 °C. The rod like morphology of rare-earth metal Gd doped SnO_2 -CuO nanoparticles are clearly seen here and there. However, there is no uniform distribution of the rods. The average particle size obtained from SEM analysis is 28 nm.

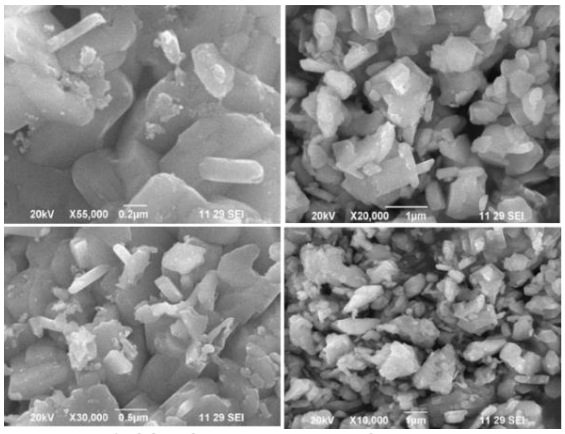

Fig. 16 SEM image of Gd doped SnO_2-CuO nanoparticles

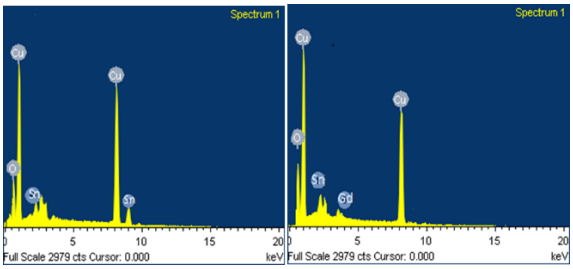

Fig. 17 EDX spectrum of synthesised (a) pure and (b) rare-earth metal Gd doped SnO_2-CuO nanoparticles

https://doi.org/10.30799/jnst.152.18040505

Cite this Article as: L. Prakash, C. Tirupathi, Synthesis and characterization of pure and rare-earth metal Gd doped SnO_2-CuO nanoparticles by co-precipitation method, J. Nanosci. Tech. 4(5) (2018) 478–482.

3.6 Energy Dispersive X-Ray Analysis (EDX)

Fig. 17 shows the EDX spectrum of pure and doped rare-earth metal SnO_2-CuO nanostructure nanoparticles. The presence of Gd is clearly seen in Fig. 17(b). This confirms that rare earth metal doping has been successfully performed into the SnO_2-CuO matrix.

4. Conclusion

Pure and rare-earth metal Gd doped SnO_2-CuO nanoparticles of 15 nm and 18 nm, average size is prepared successfully. Particles size of Gd Doped SnO_2-CuO is establish to be the higher than that of pure SnO_2-CuO nanoparticles. Optical band gap value is 5.08 eV for pure SnO_2-CuO nanoparticle and 5.14 eV for Gd doped SnO_2-CuO nanoparticle which is more in comparison to earlier reported works (4.16 eV). Surface morphology of pure and Gd doped SnO_2-CuO nanoparticles annealed at 400 °C shows that most of the particles are rod shaped and hence it may have better sensitivity. Dielectric constant of Gd doped SnO_2-CuO nanoparticles is found to be larger than that of pure SnO_2-CuO(composite) nanoparticles due to larger volume fraction of the interfaces and stronger space charge polarization (SCP) of nanoparticles. Dielectric constant and dielectric loss decrease with increased frequency (logF) at 100 °C and 200 °C. Dielectric loss shows an anomaly at around 0-3 MHz due to nano-size of the particles. The electrical-conductivity is rising with temperature reveals mobility of charge carriers responsible for hopping. As frequency (logF) increases mobility of hopping ions decreases thereby decreasing conductivity.

References

[1] K.S. Lee, M.A. El-Sayed, Gold and silver nanoparticles in sensing and imaging: sensitivity of plasmon response to size, shape, and metal composition, J. Phys. Chem. B 110(39) (2006) 19220–19225.

[2] S. Seung-Deok, J. Yun-ho, L. Seng Hun, S. Hyun-Woo, K. Dong-Wan, Low-temperature synthesis of CuO-interlaced Nano discs for lithium ion battery electrodes, Nanoscale Res. Lett. 6 (2011) 394-397.

[3] X. Zhang, D. Zhang, X. Ni, H. Zheng, Optical and electrochemical properties of nanosized CuO via thermal decomposition of copper oxalate, Solid State Electron. 52 (2008) 245-248.

[4] N. Topnani, S. Kushwaha, Wet synthesis of copper oxide nanopowder, Int. J. Green Nanotech. Mater. Sci. Eng. 1 (2009) 67-73.

[5] H. Zhang, M. Zhang, synthesis of CuO nanocrystalline and their application as electrode materials for capacitors, Mater. Chem. Phys. 108 (2008) 184-187.

[6] B. Thangaraju, Structural and electrical studies on highly conducting spray deposited fluorine and antimony doped SnO_2 thin films, Thin Solid Films 402 (2002) 71-78.

[7] D. Varshney, K. Verma, Effect of stirring time on size and dielectric properties of SnO_2 nanoparticles prepared by co-precipitation method, J. Mol. Struct. 1034 (2012) 216-222.

[8] Y. Feng, J. Wei-Xiao, H. Bao-Jun, C. Xin-lain, L. Feng, L. Ping, The magnetic and optical properties of 3d transition metal doped SnO_2 nanosheets, RSC Adv. 5 (2015) 24306-24312.

[9] N. Wan, T. Zhao, S. Sun, Q. Wu, Y. Bai, Nickel and nitrogen co doped tin dioxide Nano-composite as a potential anode material for lithium-ion batteries, Electrochem. Acta 143 (2014) 257-264.

[10] N. Hoa Hong, A. Ruyter, W. Prellier, J. Sakai, N. Huong, Magnetism in Ni-doped SnO_2 thin films, J. Phys. Condens. Matter 17 (2005) 6533-6538.

[11] M. Dehbashi, M. Aliahmad, Experimental study of structural and optical band gap of nickel doped tin oxide nanoparticles, Int. J. Phys. Sci. 7 (2012) 5415-5420.

[12] Wen-Xin Wang, Jin-Feng Wang, Hong-Cun Chen, Wen-Bin Su, Guo-Zhong Zang, Electrical nonlinearity of (Cu, Ni, Nb) - doped SnO_2 varistors system, Mater. Sci. Eng. B 99146 (2003) 457-460.

[13] F.H. Aragon, J.A.H. Coaquira, P. Hidalgo, S.W. Da Silva, S.L.M. Brito, D. Gouveac, P.C. Morais, Evidences of the evolution from solid solution to surface segregation in Ni-doped SnO_2 nanoparticles using Raman spectroscopy, J. Raman Spectros. 42 (2011) 1081-1086.

[14] A.K. Manseki, T. Sugiuraa, T. Yoshida, Microwave synthesis of size controllable SnO_2 nanocrystals for dye-sensitized solar cells, New J. Chem. 38 (2014) 596-598.

[15] Yong Wang, Jim Yang Lee, Microwave-assisted synthesis of SnO_2 - graphite nanocomposites for Li-ion battery applications, J. Power Sour. 144 (2005) 220-225.

[16] K. Kavitha, T. Subba Rao, P. Suvarna, The properties of Cu doped tin oxide and tin doped CuO, Thin Solid Films 06 (2017) 340-343.

[17] Wu. Jing, K.S. Gui , K.N. Hui, L. Li. HoHwan Chun, Y.R. Cho, Synthesis SnO_2 for sensing application, J. Sci. Electron. 27 (2016) 1719-1724.

[18] K. Sakthiraj, B. Karthikeyan, K. Balachander Kumar, Structural, optical and magnetic properties of copper (Cu) doped tin oxide (SnO_2) nanocrystal, Int. J. Chemtech. Res. 7 (2015) 1481-1487.

[19] Y. Ohtani, J. Thachibana, T. Ogura, Y. Miyaka Yakama, Synthesis of pure and doped SnO_2 for sensing behaviour, J. Alloys Compd. 279 (1998) 136-141.

[20] Honghu Zhang, Mufti Aknic, Synthesis and characterization of Gd doped magnetic nanoparticles, J. Magn. Magn. Mater. 423 (2017) 386-394.

[21] R. Sinha, S. Basu, A.K. Meikap, Investigation of the Gd doped $YCrO_3$ nanoparticles, Mater. Res. Bull. 97 (2018) 578-587.

[22] B. Poornaprakash, U. Chalapathi, S. Babu, S.H. Park, Structural, morphological optical and magnetic properties of Gd doped and Gd, Mn co-doped ZnO nanoparticles, Mater. Res. Bull. 93 (2017) 111-115.

[23] Gurpreet Singh, R. Chand Singh, Synthesis and characterization of Gd doped SnO_2 for gas sensing properties, J. Ceram. Int. 43 (2017) 2350-2360.

[24] M.A. Ming-you, H.E. Ze-Qiang, W.U. Xian Ming, Synthesis and electrochemical properties of SnO_2-CuO nanocomposite, TNM. Soc. China 16 (2006) 791-794.

[25] T. Stuchinskaya, M. Moreno, M. Cook, J. Edwards, D.R. Russell, Preparation and characterization of SnO_2 nanopowder, Photochem. Photobiol. Sci. 10 (2011) 822-831.

[26] S.D. Brown, P. Nativo, J.A. Smith, D. Stirling, P.R. Edwards, B. Venugopal, et al., Synthesis and functional analysis of CuO nanoparticles, Am. Chem. Soc. 132 (2010) 4678-4684.

https://doi.org/10.30799/jnst.152.18040505

Cite this Article as: L. Prakash, C. Tirupathi, Synthesis and characterization of pure and rare-earth metal Gd doped SnO_2-CuO nanoparticles by co-precipitation method, J. Nanosci. Tech. 4(5) (2018) 478–482.